

A UNIFIED SCALING LAW IN SPIRAL GALAXIES

JIN KODA,¹ YOSHIKI SOFUE,¹ AND KEIICHI WADA²

Received 1999 August 8; accepted 2000 January 10; published 2000 February 8

ABSTRACT

We investigate the origin of a unified scaling relation in spiral galaxies. Observed spiral galaxies are spread on a plane in the three-dimensional logarithmic space of luminosity L , radius R , and rotation velocity V . The plane is expressed as $L \propto (VR)^\alpha$ in the I passband, where α is a constant. On the plane, observed galaxies are distributed in an elongated region which looks like the shape of a surfboard. The well-known scaling relations L - V (Tully-Fisher [TF] relation), V - R (also the TF relation), and R - L (Freeman's law) can be understood as oblique projections of the surfboard-like plane into two-dimensional spaces. This unified interpretation of the known scaling relations should be a clue to understand the physical origin of all the relations consistently. Furthermore, this interpretation can also explain why previous studies could not find any correlation between TF residuals and radius. In order to clarify the origin of this plane, we simulate formation and evolution of spiral galaxies with the N -body/smoothed particle hydrodynamics method, including cooling, star formation, and stellar feedback. Initial conditions are set to 14 isolated spheres with two free parameters, such as mass and angular momentum. The cold dark matter ($h = 0.5$, $\Omega_0 = 1$) cosmology is considered as a test case. The simulations provide the following two conclusions: (1) The slope of the plane is well reproduced but the zero point is not. This zero-point discrepancy could be solved in a low-density ($\Omega_0 < 1$) and high-expansion ($h > 0.5$) cosmology. (2) The surfboard-shaped plane can be explained by the control of galactic mass and angular momentum.

Subject headings: galaxies: evolution — galaxies: formation — galaxies: kinematics and dynamics — galaxies: statistics

1. INTRODUCTION

Luminosity L , radius R , and rotation velocity V are basic parameters for spiral galaxies. We have known the correlations between each pair of them: the $\log L$ - $\log V$ (Tully & Fisher 1977), $\log V$ - $\log R$ (also Tully & Fisher 1977), and $\log R$ - $\log L$ (Freeman 1970) correlations. These scaling relations provide an observational benefit to measure galaxy distances (e.g., Strauss & Willick 1995; Giovanelli et al. 1998) and also provide theoretical benchmarks to understand the structure, formation, and evolution of spiral galaxies (e.g., Dalcanton, Spergel, & Summers 1997; Silk 1997; Mo, Mao, & White 1998).

There have been many efforts to search tighter correlations than these three. In order to improve the accuracy of distance estimation, a third-parameter effect on the Tully-Fisher (TF) relation, i.e., a correlation between TF residuals and a third parameter, has been sought by many authors (e.g., Willick et al. 1997; Courteau & Rix 1999). Most of them have concluded that the third-parameter effect may not be crucial, while Willick (1999) has found a slight dependence of TF residuals on surface brightness. On the other hand, principal component analyses have suggested that two parameters are necessary and sufficient to describe spiral galaxies (see Djorgovski 1992 for a review), in contrast to stars that are described by one parameter (mass). Kodaira (1989) has found that the correlation among all three parameters ($\log L$, $\log R$, and $\log V$) is much tighter than the correlations between any two of them. Koda & Sofue (2000) have recently found that spiral galaxies are distributed on a surfboard-shaped plane in the three-dimensional space ($\log L$, $\log R$, $\log V$). The two-dimensional scaling relations (L - V , V - R , and R - L) can be understood uniformly as oblique projections of this surfboard-shaped plane. Koda & Sofue (2000) also

argued that this unified scaling relation would be produced through galaxy formation which is affected by galactic mass and angular momentum.

Theoretically the importance of mass and angular momentum in the structure of spiral galaxies has, of course, been discussed by many authors (e.g., Fall & Efstathiou 1980; Kashlinsky 1982). Recently, the two-dimensional scaling relations (L - V , V - R , and R - L) have been discussed as the products of galaxy formation which is controlled by mass and angular momentum (Dalcanton et al. 1997; Mo et al. 1998; Koda, Sofue, & Wada 2000). In this Letter, we discuss whether the unified scaling relation (plane) in the three-dimensional space can also be a product of mass and angular momentum. We take the N -body/smoothed particle hydrodynamics (SPH) approach which includes cooling, star formation, and stellar feedback (see Tissera, Lambas, & Abadi 1997; Weil, Eke, & Efstathiou 1998; Steinmetz & Navarro 1999; Elizondo et al. 1999; Koda et al. 2000) and consider the formation of 14 galaxies with different masses and angular momenta. The simulated galaxies show internal structures as observed in spiral galaxies, e.g., the exponential density profile, flat rotation curve, and distributions of stellar age and metallicity. Using these simulated “spiral galaxies,” we try to confirm the origin of the unified scaling relation.

2. OBSERVATIONAL FACT

We briefly introduce the unified scaling relation in spiral galaxies. Throughout this Letter, we use the data set presented by Han (1992), which consists of member galaxies in 16 clusters. All of the sample galaxies in each cluster are assumed to be at the same distance indicated by the systemic recession velocities of the host cluster, which are measured in the cosmic microwave background reference frame (Willick et al. 1995). We assume $h = 0.5$, where h is the present Hubble constant in units of $100 \text{ km s}^{-1} \text{ Mpc}^{-1}$. In order to select exact members of a cluster, we reject galaxies whose recession velocities deviate more than 1000 km s^{-1} from the mean velocity of the

¹ Institute of Astronomy, University of Tokyo, Mitaka, Tokyo 181-8588, Japan.

² National Astronomical Observatory, Mitaka, Tokyo 181-8588, Japan.

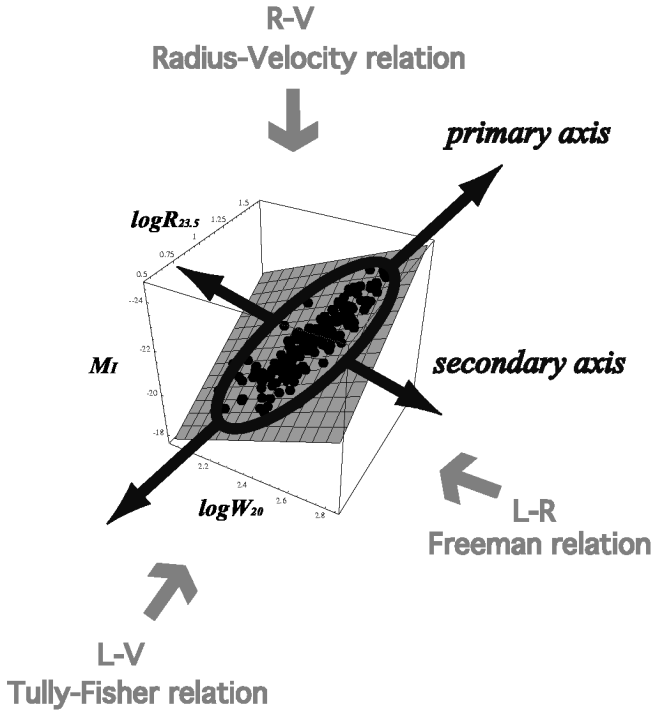


FIG. 1.—Observed spiral galaxies are distributed on a unique plane in the three-dimensional space of luminosity L , radius R , and rotation velocity V (hereafter *scaling plane*), and distributed in a surfboard-shaped (particularly elongated) region on the plane. In this schematic figure, we use the I -band absolute magnitude M_I (mag) for L , face-on isophotal radius $R_{23.5}$ (kpc) for R , and H I line width W_{20} (km s^{-1}) for V . The well-known scaling relations (L - V , V - R , and R - L) can be understood as oblique projections of the surfboard shape. The scatters of these three correlations can also be unified by the scaling plane. We hypothesize (1) that the two-dimensional distribution implies the existence of two dominant physical factors in spiral galaxy formation and (2) that one of them is more dominant than the other because of the surfboard shape.

cluster. We use total I -band magnitude M_I (in units of mag), H I velocity width W_{20} (in units of km s^{-1}), and face-on I -band isophotal radius $R_{23.5}$ (in units of kpc). Final samples consist of 177 spiral galaxies.

When we consider the three-dimensional space of luminosity L , radius R , and rotation velocity V , observed spiral galaxies are (1) distributed on a plane as $L \propto (VR)^{1.3}$ and (2) distributed in a surfboard-shaped region on the plane (Koda & Sofue 2000). Figure 1 schematically illustrates the situation with parameters of radius $\log R$, velocity $\log W$, and absolute magnitude M_I . Since the well-known two-dimensional scaling relations (L - V , V - R , and R - L) can be understood uniformly as oblique projections of this surfboard-shaped plane (Fig. 1), we hereafter call the plane *the scaling plane*. The upper panels of Figure 2 show the TF projection (left) and the edge-on projection (right) of the scaling plane. The edge-on projection has tighter correlation than the TF projection. The same plane can be found in the data sets of Mathewson, Ford, & Buchhorn (1992) and Courteau (1999) as well. Note the L - V , V - R , and R - L relations themselves may also be found as the projections of a prolate (not thin plane) distribution in a three-dimensional space. However, the plane distribution unifies the scatters of these three two-dimensional correlations as well.

In the three-dimensional space, observed galaxies are spread in the range of the order of 2 for L and the several factors for R and V . Hence, the scaling plane has exactly the elongated

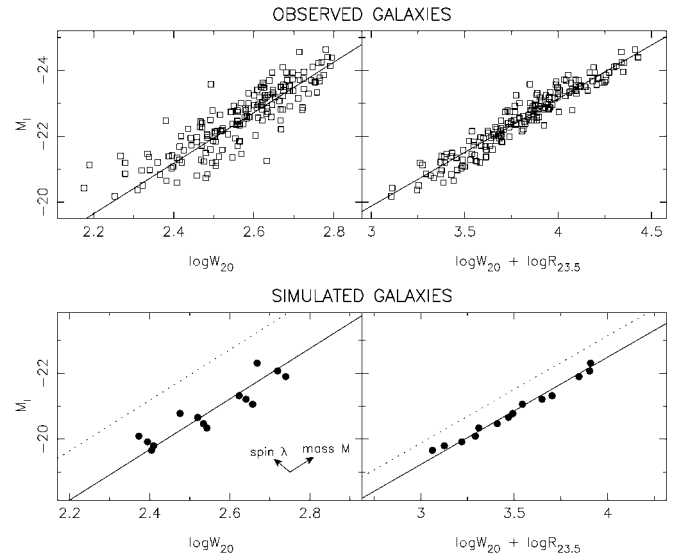


FIG. 2.—Comparison of observed (upper panels) and simulated (lower panels) galaxies in the Tully-Fisher projection (left panels) and edge-on projection (right panels) of the scaling plane. The slopes of all the lines are determined by fitting to the observation. In the lower panels, the dotted lines represent the observed correlation (as do the solid lines in the upper panels), and the zero points of the solid lines are shifted by eye to fit them to the simulations. The ranges of axes are different between upper and lower panels, but the lengths of axes are exactly the same. Hence we can compare the slope and scatter of the observations and the simulations. In the Tully-Fisher projection of simulated galaxies (lower left), the axes along mass and spin parameter are indicated by two arrows. Comparing lower left and lower right panels, we find that the scaling plane would originate from the difference of galactic mass and spin parameter.

(surfboard) shape. The primary and secondary axes are schematically illustrated in Figure 1. We hypothesize (1) that the two-dimensional distribution implies the existence of two dominant physical factors in spiral galaxy formation and (2) that one of them is more dominant than the other because of the surfboard shape.

3. NUMERICAL EXPERIMENT

3.1. Numerical Methods

We simulate formation and evolution of spiral galaxies by the N -body/SPH method similar to Katz (1992) and Steinmetz & Müller (1994, 1995). We use a GRAPE-SPH code (Steinmetz 1996), a hybrid scheme of the smoothed particle hydrodynamics and the N -body integration hardware GRAPE-3 (Sugimoto et al. 1990). This code can treat the gravitational and hydrodynamical forces, radiative cooling, star formation, and stellar feedback (see J. Koda et al. 2000, in preparation).

We take a phenomenological model of star formation. If a region is locally contracting and Jeans unstable, stars are formed at a rate $\dot{\rho}_* = c_* \rho_{\text{gas}} / \max(\tau_{\text{dyn}}, \tau_{\text{cool}})$, where ρ_* , ρ_{gas} , τ_{dyn} , and τ_{cool} are the local densities of stars and the gas, dynamical, and cooling timescales, respectively. We set $c_* = 0.05$. We assume that massive stars with mass $m \geq 8 M_\odot$ explode as Type II supernovae and release energy (10^{51} ergs), mass ($m - 1.4 M_\odot$), and metals (16% of total released mass on an average; see Nomoto et al. 1997a) into the surrounding gas at a constant rate in the first 4×10^7 yr from their birth. They leave white dwarfs with mass $1.4 M_\odot$ after the explosion. And 15% of the white dwarfs are assumed to result in Type Ia supernovae (Tsujiyama et al. 1995), which release energy (10^{51} ergs), mass

($1.4 M_{\odot}$), and metals (100% of total released mass; see Nomoto et al. 1997b) into the surrounding gas. The number of the massive stars is counted with the initial mass function (IMF) of Salpeter (1955), and we set the lower m_l and upper mass m_u of stars to $(m_l, m_u) = (0.1 M_{\odot}, 60 M_{\odot})$. The energy is released into the surrounding gas as thermal energy.

3.2. Initial Conditions

We consider 14 homogeneous spheres that are rigidly rotating, isolated, and overdense above the background field by $\delta\rho/\rho = 0.25$. The spheres follow the reduced Hubble expansion at $z = 25$ in the cold dark matter (CDM) cosmology ($\Omega_0 = 1$, $h = 0.5$ and the rms fluctuation in $8 h^{-1}$ Mpc spheres $\sigma_8 = 0.63$). Small-scale CDM fluctuations are superposed on the considered spheres. We use the same realization (random numbers) of the fluctuations for all 14 galaxies. Two free parameters, total mass M and spin parameter λ , are $M = 8 \times 10^{11} M_{\odot}$ ($\lambda = 0.10, 0.08, 0.06$), $4 \times 10^{11} M_{\odot}$ ($0.08, 0.06, 0.04$), $2 \times 10^{11} M_{\odot}$ ($0.10, 0.08, 0.06, 0.04$), and $1 \times 10^{11} M_{\odot}$ ($0.10, 0.08, 0.06, 0.04$). Since we consider collapses of isolated spheres, there is no infall of clumps at low redshift which causes an extreme transfer of angular momentum from baryons to dark matter (Navarro, Frenk, & White 1995; Steinmetz & Navarro 1999).

The gas and dark matter are represented by the same number of particles, and their mass ratio is set to 1/9 (Steinmetz & Müller 1995). The mass of a gas particle varies between 2.4×10^6 and $1.9 \times 10^7 M_{\odot}$ according to the system mass considered. The mass of a dark matter particle is between 2.1×10^7 and $1.7 \times 10^8 M_{\odot}$. Low resolution may cause artificial heating due to two-body relaxation; however, this range of particle mass is small enough to exclude the artificial heating effect (Steinmetz & White 1997). The gravitational softenings are taken to be 1.5 kpc for gas and star particles and 3 kpc for dark matter.

4. RESULTS

We compute absolute magnitude M_I of each ‘‘spiral galaxy’’ at $z = 0$ with the simple stellar population synthesis models of Kodama & Arimoto (1997) and take the isophotal radius $R_{23.5}$ (kpc) at the level 23.5 mag arcsec $^{-2}$ in the I band. The line width W_{20} (km s $^{-1}$) is derived in a way similar to observation by constructing a line-profile of gas and measuring the width at 20% level of a peak flux. All simulated galaxies have the exponential light profile and the flat rotation curve (see Koda et al. 2000).

4.1. The Scaling Plane of Simulated Galaxies

In Figure 2, we compare the observed (*upper panels*) and simulated (*lower panels*) distributions of spiral galaxies in the TF projection (*left panels*) and edge-on (*right panels*) projection of the scaling plane. In the lower panels, the dotted lines represent the observed correlations (as do the solid lines in the upper panels), and we shift the zero point of the solid lines to fit the simulations. The ranges of the figures are shifted between the upper and lower panels because of the systemic shift of simulated galaxies. The lengths of the axes, however, are exactly the same, and we can compare the slope and scatter between the upper and lower panels.

In this figure, we find the following three points: (1) The slope and scatter of both correlations are well reproduced in the simulation. Note that the slope and scatter of L - R and

R - V are also consistent with the observations. (2) The edge-on projection of the simulated scaling plane shows a much better correlation than the simulated TF projection, similar to the observations. The simulations reproduce the slope and scatter of the scaling plane well. (3) However, the distribution of simulated galaxies is systematically shifted from that of observed galaxies.

The systemic shift of the simulated distribution from the observed one amounts to $(\Delta M_I, \Delta \log R_{23.5}) = (-1.5, 0.3)$ in the three-dimensional space. This shift would result mainly from the adopted cosmology ($h = 0.5$, $\Omega_0 = 1$), which could contribute to the shift in two ways: (1) The h shifts the observed galaxies through distance estimation. If we change h from 0.5 to 1, observed galaxies are shifted by $(\Delta M_I, \Delta \log R_{23.5}) = (1.5, -0.3)$, which are sufficient to explain the above shift. (2) The lower Ω_0 would increase the ratio of baryon to dark matter and then decrease the mass-to-light ratio. If we decrease Ω_0 , simulated galaxies would be shifted in the direction of $\Delta M_I < 0$ and $\Delta \log R_{23.5} > 0$. (Note on the contrary, if we assume a lower baryon fraction in galaxies than the one adopted here, the simulated galaxies would be shifted in the opposite direction.)

In our simulations, the procedure of galaxy formation and evolution is not affected so much by changing the cosmology since we consider initial conditions of nearly monolithic collapse. Hence the comparison only in simulated galaxies would be possible even though the zero point is shifted.

4.2. Origin of The Scaling Plane

As discussed in § 2, the scaling plane has the primary and secondary axes. Here we show that these two axes of the simulated scaling plane correspond to galactic mass and angular momentum, respectively. In order for these two parameters to correspond to the primary and secondary axes exactly, they must satisfy the following three conditions: (1) The axes along these two parameters are on the scaling plane. (2) These axes are not parallel each other. (3) The axis along mass (angular momentum) is parallel to the primary (secondary) axis. In Figure 2, the lower right-hand panel shows the edge-on projection. All the simulated galaxies, which have different mass and angular momentum, lie on the same scaling plane. Condition 1 is satisfied. The axes along mass and angular momentum are illustrated in the lower left-hand panel of Figure 2 (see also Koda et al. 2000). In this TF projection, the axes along mass and angular momentum (spin parameter) are not parallel each other, which satisfies condition 2. It is clear that the projections of the primary and secondary axes onto the TF plot are along the directions of mass and angular momentum, respectively, satisfying condition 3. We conclude that the scaling plane is spread by the difference of primarily galactic mass and secondarily angular momentum.

The backbone of galactic scaling relations is the virial theorem. Most of parameters would be determined on the domination of galactic mass. However, if the mass is the only parameter which determines galactic properties, galaxies would be distributed on a *line* in the three-dimensional space. The secondary factor, spin parameter, causes a slight spread in properties of disk galaxies. Then, spiral galaxies are distributed on a particularly elongated (surfboard-shaped) plane in the three-dimensional space.

In fact, spin parameter (angular momentum) affects galactic properties in the following three ways: (1) Spin parameter changes the central concentration of disks in dark matter halos.

Lower spin parameter produces relatively concentrated disks and leads to higher rotation velocities. (2) Spin parameter changes the radius of spiral galaxies. Higher spin parameter produces galaxies with larger radii. (3) Therefore, higher spin parameter produces galaxies with lower surface densities and then leads to slower star formation. It results in brighter galaxies at $z = 0$ because of the relatively younger age of their stellar component. These three effects produce the scatters of the three scaling relations (L - V , V - R , and R - L).

5. DISCUSSION

We have introduced the scaling plane (unified scaling relations) of observed spiral galaxies in the three-dimensional space of luminosity, radius, and rotation velocity and investigated a possible origin of the scaling plane. We have shown that mass primarily determines the galaxy position in the three-dimensional space, and angular momentum (spin parameter) produces a slight spread on the scaling plane. The scaling plane is originated in the galaxy formation process, controlled by mass and angular momentum. In order to clarify the uniqueness of the origin, one could further consider (1) other cosmological models (Mo et al. 1998), (2) different ratios of baryon to dark matter, (3) different mass aggregation histories (Avila-Reese, Firmani, & Hernández 1998), and (4) other modelings of star formation and feedback (Silk 1997).

Many studies have concluded that there is no correlation of TF residuals with radius and any other parameter. These results appear to deny the existence of the scaling plane. We should note, however, that the existence of the scaling plane does not imply a clear correlation between TF residuals and radius, when the plane contains any kind of scatter, e.g., observational errors or intrinsic one. The apparent discrepancy comes from a confusion of two facts, that is, spiral galaxies are distributed (1) on a plane, and (2) in a surfboard-shaped region on it (see § 2). The definition of TF residuals are affected by property 2. If the surfboard-shaped region rotates *on* the same plane,

the TF relation (projected relation) will be changed in its slope, zero point, and “the definition of residuals” as well (see Fig. 1). Hence the correlation of TF residuals with radius is strongly affected by property 2, i.e., how galaxies are distributed *on* the plane, and if the plane contains any kind of scatter such as errors in observation, the combination of property 2 and the scatter could hide property 1, i.e., the existence of the scaling plane.

Still, the scaling plane implies correlations of each scaling relation (L - V , V - R , and R - L) with surface brightness, at least in normal galaxies. It is interesting to investigate whether low surface brightness (LSB) galaxies are also distributed on the scaling plane. Zwaan et al. (1995) discussed that LSB galaxies lie on the same TF relation as normal galaxies, while O’Neil, Bothun, & Schombert (1999) have concluded that their sample of LSB galaxies does not produce the TF relation. So, the question is still under debate, and further research would be necessary to discuss LSB galaxies in analyses of the scaling plane. There have been studies which concluded that the Freeman’s law would be an artifact due to observational selection effects, because LSB galaxies deviate from the luminosity-radius relation of normal galaxies (recently, de Jong 1996; Scorza & van den Bosch 1998). The scaling plane is so tight that the plane itself would not be an artifact due to selection effects. However, the galaxy distribution on the plane may change if selection effects affect the sample. LSB galaxies may provide a clue to understand such selection effects if they are the sequence of normal galaxies.

Numerical computations were carried out on the GRAPE system at the Astronomical Data Analysis Center of the National Astronomical Observatory, Japan. We would like to thank N. Arimoto for providing us with the tables of the stellar population synthesis. We are grateful to the anonymous referee for his/her fruitful comments. J. K. thanks the Hayakawa Fund of the Astronomical Society of Japan. J. K. also thanks Mrs. M. Redmond for reading the manuscript.

REFERENCES

- Avila-Reese, V., Firmani, C., & Hernández, X. 1998, *ApJ*, 505, 37
 Courteau, S. 1999, preprint (astro-ph/9903297)
 Courteau, S., & Rix, H. W. 1999, *ApJ*, 513, 561
 Dalcanton, J., Spergel, D. N., & Summers, F. J. 1997, *ApJ*, 482, 659
 de Jong, R. S. 1996, *A&A*, 313, 45
 Djorgovski, S. 1992, in *Morphological and Physical Classification of Galaxies*, ed. G. Longo, M. Capaccioli, & G. Busarello (Dordrecht: Kluwer), 337
 Elizondo, D., Yepes, G., Kates, R., Müller, V., & Klypin, A. 1999, *ApJ*, 515, 525
 Fall, S. M., & Efstathiou, G. 1980, *MNRAS*, 193, 189
 Freeman, L. C. 1970, *ApJ*, 160, 811
 Giovanelli, R., Haynes, M. P., Salzer, J. J., Wegner, G., da Costa, L. N., & Freudling, W. 1998, *AJ*, 116, 2632
 Han, M. 1992, *ApJS*, 81, 35
 Kashlinsky, A. 1982, *MNRAS*, 200, 585
 Katz, N. 1992, *ApJ*, 391, 502
 Koda, J., & Sofue, Y. 2000, *ApJ*, submitted
 Koda, J., Sofue, Y., & Wada, K. 2000, *ApJ*, in press
 Kodaira, K. 1989, *ApJ*, 342, 122 (K89)
 Kodama, T., & Arimoto, N. 1997, *A&A*, 320, 41
 Mathewson, D. S., Ford, V. L., & Buchhorn, M. 1992, *ApJS*, 81, 413
 Mo, H. J., Mao, S., & White, S. D. M. 1998, *MNRAS*, 295, 319
 Navarro, J. F., Frenk, C. S., & White, S. D. M. 1995, *MNRAS*, 275, 56
 Nomoto, K., et al. 1997a, *Nucl. Phys. A*, 616, 79
 ———. 1997b, *Nucl. Phys. A*, 621, 467
 O’Neil, K., Bothun, G. D., & Schombert, J. 1999, preprint
 Salpeter, E. F. 1955, *ApJ*, 121, 161
 Scorza, C., & van der Bosch, F. C. 1998, *MNRAS*, 300, 469
 Silk, J. 1997, *ApJ*, 481, 703
 Steinmetz, M. 1996, *MNRAS*, 278, 1005
 Steinmetz, M., & Müller, E. 1994, *A&A*, 281, L97
 ———. 1995, *MNRAS*, 276, 549
 Steinmetz, M., & Navarro, J. F. 1999, *ApJ*, 513, 555
 Steinmetz, M., & White, S. D. M. 1997, *MNRAS*, 288, 545
 Strauss, M. A., & Willick, J. A. 1995, *Phys. Rep.*, 261, 271
 Sugimoto, D., Chikada, Y., Makino, J., Ito, T., Ebisaki, T., & Umemura, M. 1990, *Nature*, 345, 33
 Tissera, P. B., Lambas, D. G., & Abadi, M. G. 1997, *MNRAS*, 286, 384
 Tsujimoto, T., Nomoto, K., Yoshii, Y., Hashimoto, M., Yanagida, S., & Thielemann, F.-K. 1995, *MNRAS*, 277, 945
 Tully, R. B., & Fisher, J. R. 1977, *A&A*, 54, 661 (TF)
 Weil, M. L., Eke, V. R., & Efstathiou, G. 1998, *MNRAS*, 300, 773
 Willick, J. A. 1999, *ApJ*, 516, 47
 Willick, J. A., Courteau, S., Faber, S. M., Burstein, D., & Dekel, A. 1995, *ApJ*, 446, 12
 Willick, J. A., Courteau, S., Faber, M., Burstein, D., Dekel, A., & Strauss, M. A. 1997, *ApJS*, 109, 333
 Zwaan, M. A., van der Hulst, J. M., de Block, W. J. G., & McGaugh, S. S. 1995, *MNRAS*, 273, L35